Spectral, Kinetics, and Theoretical Studies of Radical Cations Derived from Thioanisole and Its Carboxylic Derivative

Anna Korzeniowska-Sobczuk,[†] Gordon L. Hug,*[,‡] Ian Carmichael,[‡] and Krzysztof Bobrowski*[,†,§]

Institute of Nuclear Chemistry and Technology, Dorodna 16, 03-195 Warsaw, Poland, Radiation Laboratory, University of Notre Dame, Notre Dame, Indiana 46556

Received: April 24, 2002; In Final Form: July 3, 2002

Hydroxyl radicals (•OH) react with thioanisole (Ph−S−CH_3) via two competitive addition pathways: with the thioether functionality and with the aromatic ring. At neutral pH, •OH addition leads to the prompt formation of monomeric sulfur radical cations (Ph−$S^{+\bullet}$−CH_3, addition to the thioether group) and hydroxycyclohexadienyl radicals (Ph•−(OH)−S−CH_3, addition to the aromatic ring). The latter radicals subsequently decay into products, which do not include the corresponding radical cations with delocalized positive charge on the aromatic ring ($Ph^{+\bullet}$−S−CH_3). On the other hand, at low pH, •OH addition, both to the thioether functionality and to the aromatic ring, leads promptly only to Ph−$S^{+\bullet}$−CH_3 radical cations. These observations are rationalized in terms of the highly unstable nature of $Ph^{+\bullet}$−S−CH_3 radical cations (formed via proton-catalyzed water elimination from Ph•−(OH)−S−CH_3 radicals) and their rapid conversion into Ph−$S^{+\bullet}$−CH_3 radical cations. Additional experimental support for the instability of radical cations derived from aromatic thioethers with delocalized positive charge on the aromatic ring has been obtained from the •OH-induced oxidation studies of phenylthioacetic acid (Ph−S−CH_2−COOH). At low pH, Ph−S−CH_2−COOH undergoes nearly complete (relative to the available •OH radicals) quantitative decarboxylation, in contrast to neutral pH, at which the yield of decarboxylation accounts for only half of the available •OH radicals. To support our conclusions, quantum mechanical calculations were performed using density functional theory (DFT) that provided predictions of the electronic structure and optical excitation energies of the Ph−$S^{+\bullet}$−CH_3 radical cations and other key transients.

Introduction

Considerable attention has been devoted to the chemistry of sulfur-centered radicals and radical cations because of their importance as intermediates in many chemical processes including those of organic synthesis[1−3] and environmental[4−6] and biological significance.[7,8] Most of the information on sulfur-centered radical cations has come from those derived from aliphatic thioethers (R_2S).[9−13] These chemical systems have been studied extensively by electron paramagnetic resonance (EPR)[14,15] and time-resolved techniques such as pulse radiolysis[16−19] and laser flash photolysis.[20−22] An important feature of monomeric sulfur radical cations derived from aliphatic thioethers is their propensity to form relatively stable dimeric radical cations through the reaction of the monomeric radical cations with the neutral parent molecule (reaction 1).

$$R_2S^{+\bullet} + R_2S \rightleftarrows (R_2S\therefore SR_2)^+ \quad (1)$$

These dimeric intermediates are characterized by two-center, three-electron bonds.[10,11,23,24] A convenient method to form dimeric sulfur radical cations is by one-electron oxidation of aliphatic thioethers using •OH radicals[16,19,25−30] through a complex reaction mechanism that includes a hydroxysulfuranyl radical (reactions 2−5).

$$R_2S + {}^{\bullet}OH \rightarrow R_2S^{\bullet}-OH \quad (2)$$

$$R_2S^{\bullet}-OH \rightleftarrows R_2S^{+\bullet} + OH^- \quad (3)$$

$$R_2S^{\bullet}-OH + R_2S \rightleftarrows (R_2S\therefore SR_2)^+ + OH^- \quad (4)$$

$$R_2S^{\bullet}-OH + H^+ \rightarrow R_2S^{+\bullet} + H_2O \quad (5)$$

At low pH and at high [R_2S], reactions 3 and 5 are followed by reaction 1.

On the other hand, sulfur-centered radical cations derived from aromatic thioethers (ArS) have been investigated much less extensively. To the best of our knowledge only a few publications have been concerned with studies of aromatic thioethers where radical cations were generated either photochemically[31−33] or radiolytically.[34−39] It has recently been shown[34] that oxidation of selected aromatic thioethers using $SO_4^{\bullet-}$ or Tl^{2+}, results in the formation of sulfur monomeric radical cations ($ArS^{+\bullet}$). However, no dimeric sulfur radical cations ($(ArS\therefore SAr)^+$) were formed because of the spin delocalization onto the aromatic ring.[34] In opposition, it has been proposed that •OH-induced oxidation of thioanisole[35] and 2-(phenylthio)ethanol[36] leads to monomer radical cations with a positive charge localized on the benzene ring ($Ar^{+\bullet}S$) in addition to sulfur-centered dimeric radical cations ($(ArS\therefore SAr)^+$).

* To whom correspondence should be addressed.
† Institute of Nuclear Chemistry and Technology.
‡ University of Notre Dame.
§ Fax: (048-22)-811-1532. E-mail: kris@orange.ichtj.waw.pl.

10.1021/jp021039o CCC: $22.00
Published on Web 09/14/2002

In light of this controversy, it is of interest to reexamine the nature of intermediate species formed during the oxidation of aromatic thioethers. In this paper, we report the results of pulse- and γ-radiolysis studies of thioanisole (Ph−S−CH_3) and its carboxylic derivative, phenylthioacetic acid (Ph−S−CH_2−COOH), in aqueous solutions. Particular emphasis is placed on •OH-induced oxidation because it allows a detailed quantification of the relative contribution of the •OH addition to the benzene ring and to the thioether functionality. Furthermore, to support our conclusions, quantum mechanical calculations were performed using density functional theory (DFT) to elucidate the structure of some of the key transients proposed herein and to calculate the location and strength of their associated optical absorptions.

Experimental Section

Materials. Thioanisole (TA) was purchased from Aldrich Chemical Co. (Milwaukee, WI), and (phenylthio)acetic acid was obtained from Lancaster (Pelham, NH). All chemicals were of the purest commercially available grade and were used as received. Potassium peroxydisulfate ($K_2S_2O_8$) was from Sigma Chemical Company (St. Louis, MO). Solutions were made with deionized water (18 MΩ resistance) provided by a Millipore Milli-Q system. The pH was adjusted by the addition of either NaOH or $HClO_4$. Solutions were subsequently purged for at least 30 min per 500 mL of sample with the desired gas (N_2O, N_2, or O_2) before pulse irradiation and for 15 min per 5 mL of sample with N_2O before γ-irradiation.

Pulse Radiolysis. Pulse radiolysis experiments were performed with the Notre Dame 8 MeV Titan Beta model TBS 8/16-1S linear electron accelerator and the Lodz Technical University 6 MeV ELU-6 linear electron accelerator with typical pulse lengths of 2−10 and 5−17 ns, respectively. Detailed descriptions of the experimental setups have been given elsewhere along with the basic details of equipment and data collection systems at the Notre Dame Radiation Laboratory[40] and Lodz Technical University.[41,42] Absorbed doses per pulse were on the order of 2−10 Gy (1 Gy = 1 J kg^{-1}). Dosimetry was based on N_2O-saturated solutions containing 10^{-2} M KSCN, taking a radiation chemical yield of $G = 6.13$ (0.635 μM J^{-1}) and a molar extinction coefficient of 7580 M^{-1} cm^{-1} at 472 nm for the $(SCN)_2^{\bullet-}$ radical.[43] For practical purposes, the G-unit rather than the SI-unit for radiation chemical yields is used throughout this paper. The G-unit denotes the number of species formed or converted per 100 eV of absorbed energy; $G = 1.0$ corresponds to 0.1036 μmol J^{-1} of absorbed energy in aqueous solutions.[44] Experiments were performed with a continuous flow of the sample solutions at room temperature (∼23 °C). Experimental error limits are ±10% unless specifically noted.

γ Radiolysis. The γ-radiolysis experiments were carried out in the field of a ^{60}Co γ source (Issledovatel, USSR) at the Institute of Nuclear Chemistry and Technology (Warsaw, Poland). The dose rates were determined with Fricke dosimetry.[45] The applied radiation doses were adjusted so that the radiolytic conversion of the starting material was <15% to avoid secondary reactions of radiolytically produced radicals with the reaction products.

Gas Chromatographic Analysis of CO_2. The quantitative CO_2 analysis was achieved using the gas chromatographic headspace technique using a Shimadzu 14B gas chromatograph equipped with a thermal conductivity detector. CO_2 was separated from N_2O on a Porapak Q column with helium as the carrier gas.

Radiolysis of Water. The radiolysis of water leads to the formation of the primary reactive species shown in reaction 6.[44]

$$H_2O \rightarrow {}^{\bullet}OH,\ e_{aq}^{-},\ {}^{\bullet}H \qquad (6)$$

In N_2O-saturated solutions ($[N_2O]_{sat} \approx 2 \times 10^{-2}$ M),[43] the hydrated electrons, e_{aq}^{-}, are converted into •OH radicals according to eq 7 ($k_7 = 9.1 \times 10^9$ M^{-1} s^{-1}).[43] Reaction 7 nearly

$$e_{aq}- + N_2O + H_2O \rightarrow {}^{\bullet}OH + OH^- + N_2 \qquad (7)$$

doubles the amount of •OH radicals available for reaction with substrates. The effective radiation chemical yields, G, of the primary species available for the reaction with a substrate depend on the concentration of the added substrate. For N_2O-saturated solutions, the effective radiation chemical yield of •OH radicals converting a given substrate into substrate-derived radicals can be calculated on the basis of the formula given by Schuler et al.[46] This formula relates the G-value of substrate radicals to the product of the rate constant for the reaction of •OH radicals with the substrate and the substrate concentration itself. At pH < 4 the diffusion-controlled reaction of e_{aq}^{-} with protons becomes important (reaction 8, $k_8 = 2.0 \times 10^{10}$ M^{-1} s^{-1})[47]

$$e_{aq}^{-} + H^+ \rightarrow {}^{\bullet}H \qquad (8)$$

resulting in a pH-dependent lowered yield of •OH radicals and a correspondingly increased yield of •H atoms. For the selective monitoring of the reaction of •OH radicals with a substrate at very low pH, the solution was saturated with oxygen. Under these conditions, •H atoms are rapidly converted into perhydroxyl radicals according to eq 9 ($k_9 = 2.1 \times 10^{10}$ M^{-1} s^{-1}).[47]

$$ {}^{\bullet}H + O_2 \rightarrow {}^{\bullet}HO_2 \qquad (9)$$

To study the reaction between •H atoms and a substrate, the solutions were acidified to pH 1, and 0.5 M 2-methyl-2 propanol (*tert*-butyl alcohol, *t*-BuOH) was added to the solution to scavenge the •OH radicals (reaction 10, $k_{10} = 6.8 \times 10^8$ M^{-1} s^{-1})[47]

$$ {}^{\bullet}OH + (CH_3)_3COH \rightarrow {}^{\bullet}CH_2(CH_3)_2-COH + H_2O \qquad (10)$$

Sulfate radical anions ($SO_4^{\bullet-}$) were also used as oxidizing species to convert a substrate into the corresponding radical cations. The $SO_4^{\bullet-}$ radical anions were produced in Ar-saturated solutions containing $S_2O_8^{2-}$ and *tert*-butyl alcohol at pH 5.5−6.0. Under these conditions, the $SO_4^{\bullet-}$ radical anions are formed according to eq 11 ($k_{11} = 1.2 \times 10^{10}$ M^{-1} s^{-1}).[47] •OH radicals

$$e_{aq}^{-} + S_2O_8^{2-} \rightarrow SO_4^{\bullet-} + SO_4^{2-} \qquad (11)$$

do not interfere with the measurement because of reaction 10.

Computational Details

Density functional theory calculations were performed with the Gaussian 98 electronic structure software package[48] employing the popular B3LYP functional.[49] This hybrid functional comprises both local[50] and nonlocal[51] (gradient-corrected) exchange and correlation[52,53] contributions mixed with a piece of exact (Hartree−Fock) exchange. The mixing parameters were derived from fits to known thermochemistry of a well-characterized set of small molecules. For open-shell systems (the transient radicals and radical cations), spin-unrestricted DFT (UB3LYP) was employed. For structural studies, the (heavy-

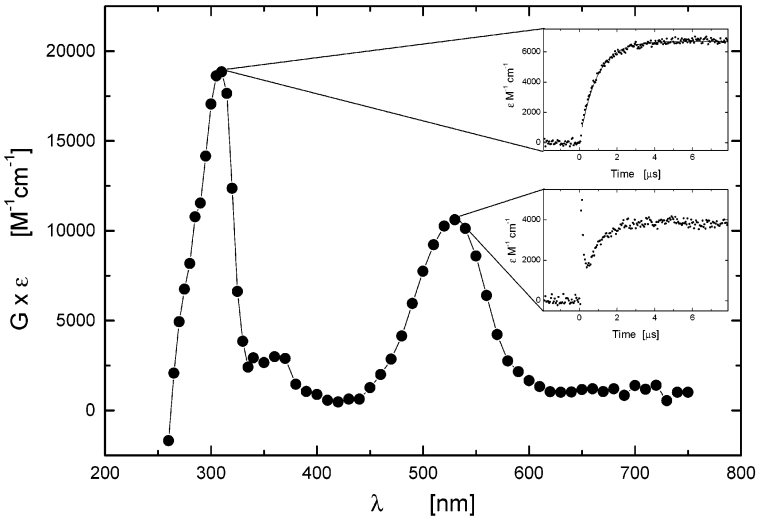

Figure 1. Transient absorption spectrum recorded after pulse irradiation of an Ar-saturated aqueous solution containing 0.2 mM thioanisole (TA), 2 mM $K_2S_2O_8$, and 0.1 M *tert*-butyl alcohol 7 μs after the pulse at pH 5.6. Insets show experimental traces for the formation of the $Ph-S^{+\bullet}-CH_3$ radical cation at $\lambda = 310$ nm (top) and 530 nm (bottom).

atom) polarized split-valence 6-31G* basis set[54] was used. DFT geometries are often converged with modest basis sets in sharp contrast to the extensive basis set requirements of wave function based methods. Vertical excited states were located using time-dependent (TD) density functional response theory within the random phase approximation.[55] TD-UB3LYP performs well for valence states but has difficulties with Rydberg transitions because of the incorrect asymptotic functional behavior. To locate the absorption maxima and estimate the transition strength, diffuse functions were added to the heavy-atom basis and polarizing p functions were added to the hydrogens, 6-31+G(d,p). The characteristics of the charge distributions in the neutral and ionized species were mapped with a natural population analysis from the NBO component[56] of Gaussian 98, and the spin populations in the open-shell species were obtained from the standard Mulliken approach.

Results

Oxidation by $SO_4^{\bullet-}$ Radical Anions. *Thioanisole (TA)*. The $SO_4^{\bullet-}$ radical anion is known[34] to react with thioanisole through one-electron oxidation, forming the corresponding monomeric sulfur-centered radical cation (**1a)** (eq 12). Pulse radiolysis

$$SO_4^{\bullet-} + Ph-S-CH_3 \rightarrow Ph-S^{+\bullet}-CH_3 + SO_4^{2-} \quad (12)$$
$$(\mathbf{1a})$$

studies were carried out to generate the transient optical absorption spectrum of **1a** to obtain quantitative spectral data on **1a** with the same pulse radiolysis setup used to obtain transient optical absorption spectra formed during the $^{\bullet}OH$-induced oxidation of thioanisole. Our absorption spectrum in Figure 1 can positively identify the transient as **1a** because the overall spectrum exhibits two strong characteristic absorption maxima located at $\lambda_{max} = 310$ and 530 nm. The formation of **1a** was followed by measuring the rate of optical density increase at 310 nm (Figure 1, top inset) and 530 nm (Figure 1, bottom inset). This transient has been assigned to **1a** by Ioele et al.[34] For the specific conditions employed (TA, 0.2 mM; $S_2O_8^{2-}$, 2 mM; *tert*-butyl alcohol, 0.1 M, pH 5.6), one can assume that $G(SO_4^{\bullet-}) = 2.65$. The $SO_4^{\bullet-}$ radical anion can abstract hydrogen atoms from *tert*-butyl alcohol (eq 13, $k_{13} = 6.0 \times 10^5$ M^{-1} s^{-1})[57] as well from the methyl site of TA (eq 14, $k_{14} \approx 4.0 \times 10^8$ M^{-1} s^{-1}).[34] From eqs 12−14 with $k_{12} = 3.9 \times 10^9$ M^{-1} s^{-1},[34] calculations assuming standard competition kinetics give G(**1a**) ≈ 2.15. Division of the radiation chemical yields, expressed as $G\epsilon$, by the radiation chemical yield of $G = 2.15$, yields $\epsilon_{310} = 8800$ M^{-1} cm^{-1} and $\epsilon_{530} = 4950$ M^{-1} cm^{-1}. These values are in a very good agreement with the documented values by Ioele et al.[34]

$$SO_4^{\bullet-} + (CH_3)_3COH \rightarrow {}^{\bullet}CH_2(CH_3)_2-COH + HSO_4^- \quad (13)$$

$$SO_4^{\bullet-} + Ph-S-CH_3 \rightarrow Ph-S-{}^{\bullet}CH_2 + HSO_4^- \quad (14)$$

Phenylthioacetic Acid (PTAA). A strong transient spectrum with $\lambda_{max} = 330$ nm and $G\epsilon_{330} = 11\,200$ M^{-1} cm^{-1} was seen 7 μs after the radiolytic pulsing of an aqueous, Ar-saturated solution containing 0.2 mM phenylthioacetic acid (PTAA), 2 mM $K_2S_2O_8$, and 0.1 M *tert*-butyl alcohol at pH 6.0 (Figure 2). Taking $G(SO_4^{\bullet-}) = 2.65$, we calculate $\epsilon_{330} = 4200$ M^{-1} cm^{-1}. An analogous absorption spectrum ($\lambda_{max} = 330$ nm, $\epsilon_{330} = 3800$ M^{-1} cm^{-1}) was observed as a result of the dehydrogenation of thioanisole (TA) by oxide radical anions ($O^{\bullet-}$) and was assigned to the $PhSC^{\bullet}H_2$ radical.[34] Thus, it can be concluded that PTTA undergoes complete (relative to the available $SO_4^{\bullet-}$ radical anions) quantitative decarboxylation. Because in our absorption spectrum in Figure 2 we were not able positively to assign any absorption band to a precursor of $PhSC^{\bullet}H_2$ in the PTAA oxidation by $SO_4^{\bullet-}$, that is, $Ph-S^{+\bullet}-CH_2-COO^-$ (**1b**), we suggest that this sulfur-centered radical cation is very unstable and decays on the submicrosecond time range, forming the $PhSC^{\bullet}H_2$ radical (Figure 2, inset).

Oxidation by $^{\bullet}OH$ Radicals. *Thioanisole (TA)*. The pulse radiolysis of aqueous, N_2O-saturated solutions containing 1 mM thioanisole (TA) at pH 6.7 yields a complex spectrum of transients with absorption maxima at $\lambda_{max} = 310$, 365, and 530 nm with the respective $G\epsilon = 31\,550$, 16 800, and 15 400 M^{-1} cm^{-1} (Figure 3). The 310- and 530-nm absorption bands were attributed accordingly to the monomeric sulfur radical cations ($Ph-S^{+\bullet}-CH_3$) (**1a**) by comparison to the spectrum of the species formed from TA by electron transfer to $SO_4^{\bullet-}$. The 365-nm absorption band was assigned to a species formed by an $^{\bullet}OH$ radical addition to the benzene ring ($Ph^{\bullet}-(OH)-S-CH_3$) (**2a**). The formation of **1a** was followed by measuring the rate of optical density increase at 310 nm (Figure 3, top left inset) and 530 nm (Figure 3, bottom inset). The formation of **2a** was

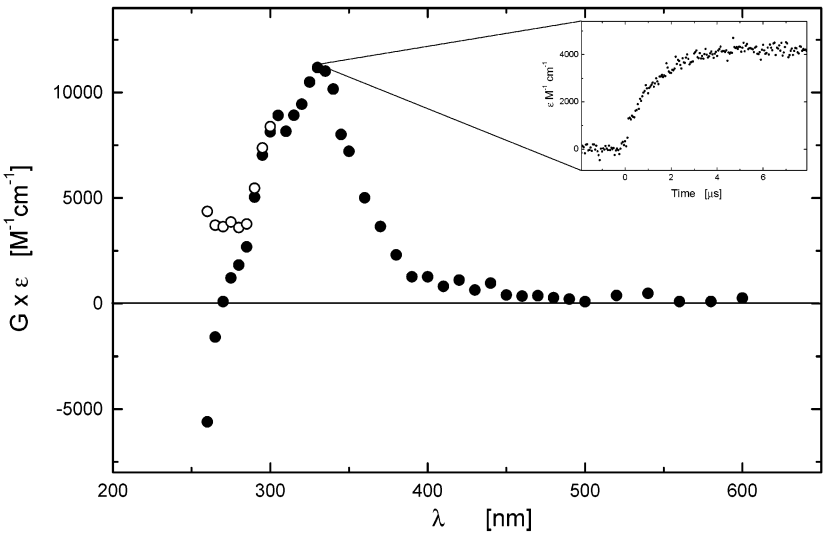

Figure 2. Transient absorption spectrum recorded after pulse irradiation of an Ar-saturated aqueous solution containing 0.2 mM phenylthioacetic acid (PTAA), 2 mM $K_2S_2O_8$, and 0.1 M *tert*-butyl alcohol 7 μs after the pulse at pH 6.0: (●) exprimental spectrum, (○) spectrum corrected for loss of the absorbance of the parent compound. Inset shows the experimental trace for the formation of the Ph−S−CH_2• radical at $\lambda = 330$ nm.

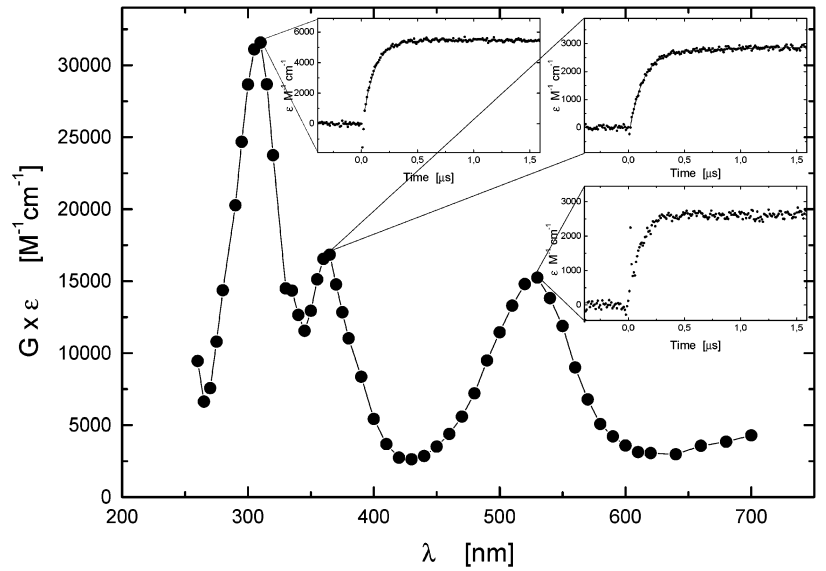

Figure 3. Transient absorption spectrum recorded after pulse irradiation of an N_2O-saturated aqueous solution containing 1 mM thioanisole (TA) 1.4 μs after the pulse at pH 6.7. Insets show experimental traces for the formation of the Ph−S^{+}•−CH_3 radical cation at $\lambda = 310$ nm (top left) and at $\lambda = 530$ nm (bottom) and hydroxycyclohexadienyl radical (Ph•−(OH)−S−CH_3) at $\lambda = 365$ nm (top right).

followed by measuring the rate of optical density increase at 365 nm (Figure 3, right top inset). The *G*-value of •OH radicals that react with the given TA concentration (1 mM) was calculated as 5.6 on the basis of the formula of Schuler et al.[46] using the recently redetermined rate constant for the reaction of TA with •OH radicals (9.90×10^9 M^{-1} s^{-1}).[4] Division of $G\epsilon$ by the maximum radiation chemical yield of G(•OH) = 5.6 yields apparent extinction coefficients of $\epsilon_{310} = 5650$ M^{-1} cm^{-1}, $\epsilon_{365} = 3000$ M^{-1} cm^{-1}, and $\epsilon_{530} = 2750$ M^{-1} cm^{-1}.

Because the 530-nm absorption band does not overlap with the absorption bands of the other species, one can calculate immediately the fraction of the •OH radicals that induced oxidation of the thioether functionality, leading to Ph−S^{+}•−CH_3 radical cations. To account for this contribution, the 530 nm absorption (with an apparent extinction coefficient of ϵ_{530} = 2750 M^{-1} cm^{-1}) was divided by the previously calculated extinction coefficient of the Ph−S^{+}•−CH_3 radical cation (ϵ_{530} = 4950 M^{-1} cm^{-1}) (see Figure 1). The resulting value of ∼0.55 represents the contribution to the transient spectrum from one of the two competitive •OH addition pathways, that is, reaction with the thioether functionality. For the radical cation **1a**, the ratio of the optical densities at 310 nm vs 530 nm can be calculated from the ratios of the corresponding extinction coefficients (8800:4950) in the $SO_4^{\bullet-}$ -induced oxidation of TA (see Figure 1). The contribution of the radical cation **1a** to the 310-nm absorption in the transient spectrum following the •OH-induced oxidation of TA can, therefore, be calculated as 8800/4950 × 2750 M^{-1} cm^{-1} = 4900 M^{-1} cm^{-1}. Because the absorption bands at 310 and 365 nm overlap strongly, the resulting residual absorption at 310 nm (5650 M^{-1} cm^{-1} − 4900 M^{-1} cm^{-1} = 750 M^{-1} cm^{-1}) can be assigned as mostly belonging to the hydroxycyclohexadienyl radical (Ph•−(OH)−S−CH_3) (**2a**).

Several corrections also had to be made for the 365-nm absorption because the absorption of **1a** contributes to the overall absorption at that wavelength. The ratio for the absorption of radical cation **1a** at 365 nm versus that at 310 nm was estimated as 500:8800 from the work of Ioele et al.[34] in which Ph−S^{+}•−CH_3 radical cations were generated from the corresponding sulfoxide. Taking $\epsilon_{310} = 4900$ M^{-1} cm^{-1} as the contribution

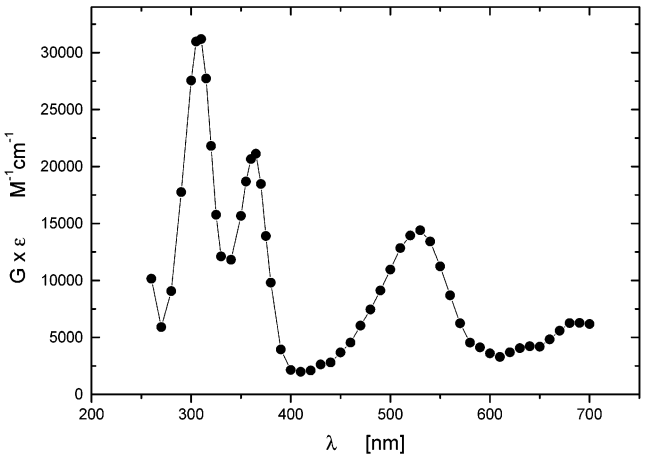

Figure 4. Transient absorption spectrum recorded after pulse irradiation of an N_2-saturated aqueous solution containing 1 mM thioanisole (TA) 1.4 μs after the pulse at pH 0.

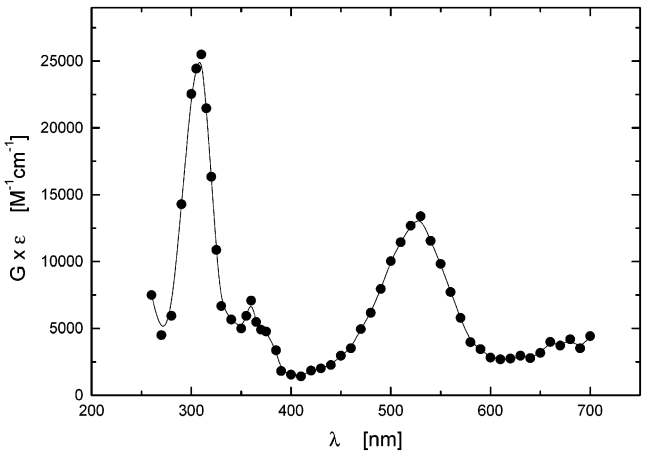

Figure 5. Transient absorption spectrum recorded after pulse irradiation of an O_2-saturated aqueous solution containing 1 mM thioanisole (TA) 200 ns after the pulse at pH 0.

from **1a** and multiplying by the factor (500/8800) gives the contribution of **1a** to the 365-nm transient absorption in Figure 3. Removing this from the overall apparent ϵ_{365} leaves 2720 M^{-1} cm^{-1}. This residual apparent ϵ_{365} still has contributions from both the $^{\bullet}$H atom adduct to the aromatic ring of thioanisole[4] (formed in reaction 15) and from the hydroxycyclohexadienyl radicals.

$$H + Ph{-}S{-}CH_3 \rightarrow Ph^{\bullet}(H){-}S{-}CH_3 \quad (\mathbf{3a}) \qquad (15)$$

The $^{\bullet}$H atom contribution can be estimated because $^{\bullet}$H atoms are present at a 10% yield relative to $^{\bullet}$OH radicals in N_2O-saturated solutions. Taking the extinction coefficient for $Ph^{\bullet}{-}(H){-}S{-}CH_3$ radicals (**3a**) as $\epsilon_{365} = 6200$ M^{-1} cm^{-1}, reestimated in this work (vide infra), the **3a** contribution to the overall 365-nm absorption can be removed. When this is taken into account, the remaining apparent extinction coefficient of 2100 M^{-1} cm^{-1} at 365 nm is associated only with hydroxycyclohexadienyl radicals (**2a**). If this apparent extinction coefficient is divided by 0.45 (the fraction of $^{\bullet}$OH reacting with the aromatic ring), one arrives at the value of $\epsilon_{365} = 4700$ M^{-1} cm^{-1} for the actual extinction coefficient of $Ph^{\bullet}{-}(OH){-}S{-}CH_3$ (**2a**). The contributions of the two competitive $^{\bullet}$OH addition pathways calculated from the spectral studies (thioether functionality (0.55) and aromatic ring (0.45)) are in excellent agreement with the rate constants determined for the respective $^{\bullet}$OH addition pathways: 9.90×10^9 M^{-1} s^{-1} (with the thioether functionality) and 7.85×10^9 M^{-1} s^{-1} (with the aromatic ring).[4]

Experiments were also performed at pH 0 to accelerate any proton-catalyzed reactions involving $^{\bullet}$OH adducts to the thioether functionality or the aromatic ring.[58−60] A transient spectrum obtained 1.4 μs after the electron pulse in N_2-saturated solutions containing 1 mM thioanisole (TA) at pH 0 exhibits a complex spectrum of transients with absorption maxima at $\lambda_{max} = 310$, 365, and 530 nm with the respective $G\epsilon = 31\,100$, 21 250, and 14 000 M^{-1} cm^{-1} (Figure 4). The 310-nm and 530-nm absorption bands were again attributed accordingly to the monomeric sulfur radical cations ($Ph{-}S^{+\bullet}{-}CH_3$). Division of $G\epsilon$ by the maximum radiation chemical yield of $G(^{\bullet}OH) = 2.8$ yields apparent extinction coefficients of $\epsilon_{310} = 11\,100$ M^{-1} cm^{-1} and $\epsilon_{530} = 5000$ M^{-1} cm^{-1}. The latter value of the apparent extinction coefficient clearly indicates that the monomeric sulfur radical cations (**1a**) are formed with 100% of the available $^{\bullet}$OH radicals because this computed apparent extinction coefficient is almost the same as the value of $\epsilon_{530} = 4950$ M^{-1} cm^{-1} as determined above for species **1a**. Thus, with no remaining $^{\bullet}$OH yield left unaccounted for, the strong 365-nm absorption band with an apparent extinction coefficient of $\epsilon_{365} = 7600$ M^{-1} cm^{-1} can be assigned exclusively to an adduct of the $^{\bullet}$H atom to the benzene ring ($Ph^{\bullet}{-}(H){-}S{-}CH_3$) (**3a**)[4] and to the $Ph{-}S^{+\bullet}{-}CH_3$ (**1a**). Corrections similar to those applied to the data from neutral solutions (vide supra) had to be made because the absorption bands at 310 and 365 nm overlap strongly. First, the contribution of the radical **1a** to the 310-nm absorption band can be calculated as $8800/4950 \times 5000$ M^{-1} $cm^{-1} = 8900$ M^{-1} cm^{-1}. The resulting residual absorption at 310 nm (11 100 M^{-1} cm^{-1} − 8900 M^{-1} $cm^{-1} = 2200$ M^{-1} cm^{-1}) can be assigned as belonging to the **3a** radical. Then, the correction for the contribution of the radical **1a** at 365-nm was calculated taking the 500/8800 factor from the work of Ioele et al.[34] and the apparent extinction coefficient $\epsilon_{310} = 8900$ M^{-1} cm^{-1} of **1a**. When the resulting apparent extinction coefficient of **1a**, 500 M^{-1} cm^{-1} at 365 nm, was then subtracted from the overall apparent extinction coefficient $\epsilon_{365} = 7600$ M^{-1} cm^{-1}, one arrives at the value of 7100 M^{-1} cm^{-1}. This last value was subsequently corrected for the maximum radiation chemical yield of $G(^{\bullet}H) = 3.2$, and the resulting value represents the extinction coefficient for $Ph^{\bullet}{-}(H){-}S{-}CH_3$ radicals (**3a**). The value of $\epsilon_{365} = 6200$ M^{-1} cm^{-1} is in fair agreement with $\epsilon_{365} = 6900$ M^{-1} cm^{-1} calculated from the work of Tobien et al.[4]

Further confirmation of the validity of the above spectra assignments was obtained from the study of O_2-saturated solutions containing 1 mM thioanisole (TA) at pH 0. Under these experimental conditions, $^{\bullet}$H atoms are predominantly scavenged by oxygen (reaction 9). From eqs 9 and 15 with $k_{15} = 3.1 \times 10^9$ M^{-1} s^{-1},[4] calculations assuming standard competition kinetics give $G(\mathbf{3a}) = 0.36$. The transient absorption spectrum observed 200 ns after the pulse is characterized by two strong absorption maxima at $\lambda_{max} = 310$ and 530 nm with the respective $G\epsilon = 25\,480$ and 13 850 M^{-1} cm^{-1} (Figure 5). The observations reported above show that the intensity of the 530-nm absorption band is not affected by the presence of oxygen, confirming the cationic character of this absorbing species. On the other hand, the intensity of the 365-nm band is strongly decreased ($G\epsilon_{365} = 3900$ M^{-1} cm^{-1}) compared to $G\epsilon_{365} = 21\,250$ M^{-1} cm^{-1} in N_2-saturated solutions (vide supra). Removing the contribution of **1a** from the overall absorption leaves $G\epsilon_{365} = 2500$ M^{-1} cm^{-1}. If this value is divided by 6200 M^{-1} cm^{-1} (the actual extinction coefficient of **3a**), one arrives with the value of $G(\mathbf{3a}) = 0.4$. Thus, the calculated radiation

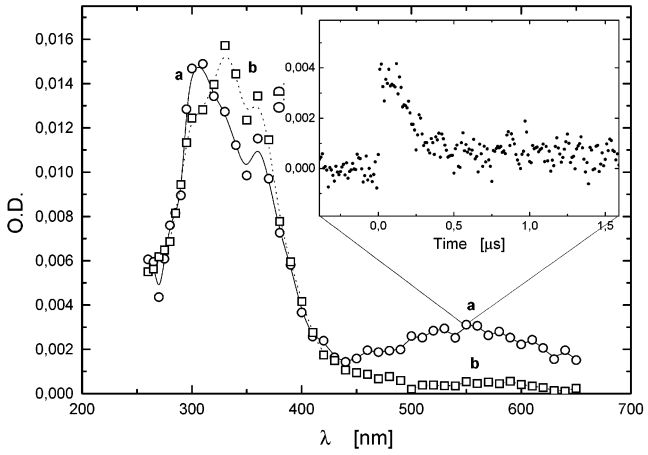

Figure 6. Transient absorption spectra recorded after pulse irradiation of an N_2O-saturated aqueous solution containing 2 mM phenylthioacetic acid (PTTA) 140 ns (curve a) and 1.4 μs (curve b) after the pulse at pH 6.97. Inset shows the experimental trace for the decay of the Ph$-S^{+\bullet}-CH_2-COO^-$ radical cation at $\lambda = 550$ nm.

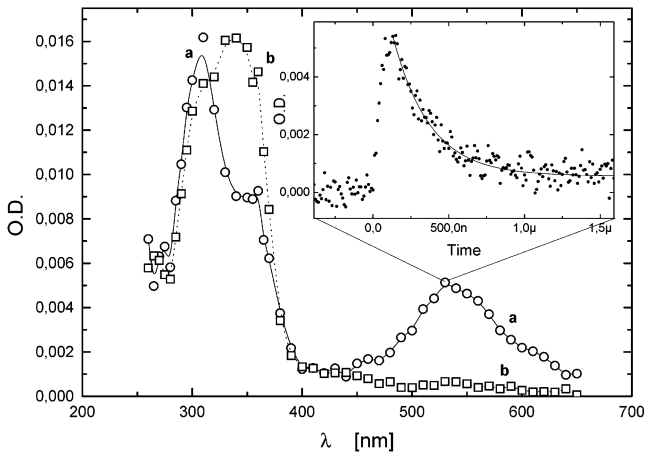

Figure 7. Transient absorption spectra recorded after pulse irradiation of an N_2-saturated aqueous solution containing 2 mM phenylthioacetic acid (PTTA) 140 ns (curve a) and 1.4 μs (curve b) after the pulse at pH 1.0. Inset shows the experimental trace for the decay of the Ph$-S^{+\bullet}-CH_2-COOH$ radical cation at $\lambda = 530$ nm.

chemical yield of **3a** is in excellent agreement with the expected radiation chemical yield based on the above calculations that assumed standard competition kinetics (vide supra).

Phenylthioacetic Acid (PTAA). The pulse irradiation of an N_2O-saturated aqueous solution, pH 6.97, containing 2 mM phenylthioacetic acid (PTAA) leads to the spectrum shown in Figure 6, curve a, observed 140 ns after the pulse. It consists of two distinct bands with $\lambda_{max} = 310$ and 550 nm, which are assigned to the monomeric sulfur radical cation ($Ph-S^{+\bullet}-CH_2-CO_2^-$) (**1b**) on the basis of the observed absorption spectrum of **1a** in thioanisole. According to our earlier suggestion (vide supra), this radical is very short-lived and decays on the hundreds of nanosecond time scale with a half-life of $t_{1/2} =$ 200 ns (inset in Figure 6). Because addition to the aromatic ring is one of the likely reaction pathways for $^\bullet$OH radicals and $^\bullet$H atoms, we have attributed the distinct 360-nm band both to hydroxycyclohexadienyl-type, $Ph^\bullet(OH)-CH_2CO_2^-$ (**2b**), and cyclohexadienyl-type radicals, $Ph^\bullet(H)-CH_2CO_2^-$ (**3b**), respectively. After decay of the $Ph-S^{+\bullet}-CH_2-CO_2^-$ radical cation (**1b**), the spectrum observed is dominated by an absorption maximum at $\lambda_{max} = 330$ nm (Figure 6, curve b). By analogy to the absorption spectrum of the product of the dehydrogenation of thioanisole by $O^{\bullet-}$ ($Ph-S-^\bullet CH_2$, $\lambda_{max} = 330$ nm),[34] we believe that this absorption is due to this same species, resulting from a decarboxylation of the $Ph-S^{+\bullet}-CH_2-CO_2^-$ radical cation. Furthermore, as shown in Figure 8 (vide infra), high yields of CO_2 were obtained in the γ radiolysis of PTAA at pH 6.9, indicating the existence of this reaction pathway.

At pH 1, the pulse irradiation of N_2-saturated solutions of 2 mM phenylthioacetic acid (PTAA) leads to the formation of 310-nm and 530-nm bands ca. 140 ns after the pulse, indicating the formation of monomeric sulfur radical cations ($Ph-S^{+\bullet}-CH_2-COOH$) (Figure 7, curve a). This radical cation is very short-lived, but its lifetime is slightly enhanced ($t_{1/2} = 250$ ns) (inset in Figure 7) compared to the lifetime of the $Ph-S^{+\bullet}-CH_2-CO_2^-$ radical (vide supra). Because experiments were carried out in very acidic solutions, in which most of the hydrated electrons are converted into $^\bullet$H atoms (reaction 8), the strong 360-nm absorption is attributed to the cyclohexadienyl-type radicals, $Ph^\bullet(H)-CH_2COOH$. We were not able to compute accurately the total radiation chemical yield, ($G(Ph-S^{+\bullet}-CH_2-COOH)$, of the monomeric sulfur radical cations because of their short lifetime and are, thus, unable to compare its yield with the total available yield of $^\bullet$OH radicals at pH 1. Therefore, a contribution of hydroxycyclohexadienyl-type radicals, $Ph^\bullet(OH)-CH_2COOH$, to the overall absorption at 360 nm cannot be ruled out. Following the decay of the $Ph-S^{+\bullet}-CH_2-COOH$ radical cations, the spectrum observed is again dominated by an absorption maximum at $\lambda_{max} = 330$ nm (Figure 7, curve b). The appearance of the 330-nm band is an indication that $Ph-S-^\bullet CH_2$ radicals are formed. These radicals are produced from the decarboxylation of $Ph-S^{+\bullet}-CH_2-COOH$ radical cations, which is, in turn, indicated by the formation of CO_2 during the γ radiolysis of PTAA at pH 1 (Figure 8, vide infra).

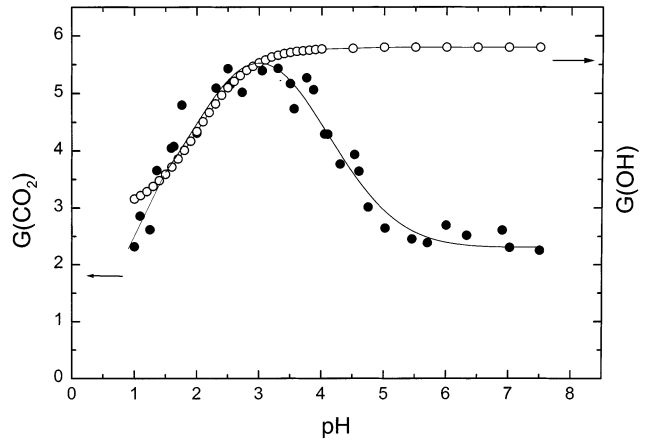

Figure 8. Plot of the final radiation chemical yields of CO_2 (●) measured after γ radiolysis of N_2O-saturated aqueous solutions containing 2 mM phenylthioacetic acid (PTTA) at various pH (for comparison, the *G*-values of $^\bullet$OH radicals (○) that can react with the given PTAA concentration (2 mM) calculated taking into account the competition between reactions 7 and 8 and the formula given by Schuler et al.).

CO_2 Formation as a Function of pH. The γ radiolysis of N_2O-saturated aqueous solutions at various pH values between 1.0 and 7.0 containing 2 mM of phenylthioacetic acid (PTAA) yields CO_2. The *G*-values were calculated from the straight lines derived by plotting the measured CO_2 concentrations vs the applied radiation dose for five or six different doses. Taking into account the competition between reactions 7 and 8, all final CO_2 yields were shown together with the *G*-values of $^\bullet$OH radicals that can react with the given PTAA concentration (2 mM) (Figure 8). Up to pH $\approx$ 3.5, the measured $G(CO_2)$ yields account for ca. 80−100% of the available $^\bullet$OH radicals. Above pH 3.5, there is a progressive decrease in $G(CO_2)$ on going from

CHART 1

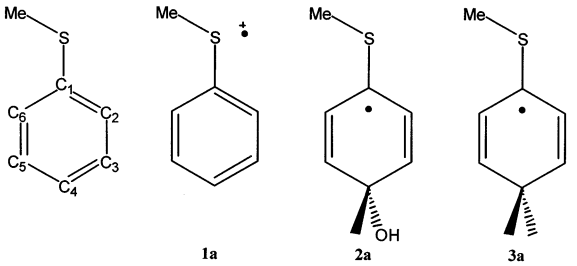

TABLE 1: Structural Parameters[a] in Thioanisole and Some Radiolytically Derived Transients

	neutral	radical cation	4-OH adduct	4-H adduct
R(S−Me)	182.2	182.0	182.3	182.4
R(S−C_1)	178.6	172.0	176.3	176.9
R(C_1−C_2)	140.5	143.2	143.1	143.1
R(C_2−C_3)	139.2	138.0	136.0	136.0
R(C_3−C_4)	139.8	140.7	150.2	150.3
R(C_4−C_5)	139.4	141.3	150.0	150.3
R(C_5−C_6)	139.8	138.0	136.7	136.6
R(C_6−C_1)	140.0	142.3	142.2	142.3
ϑ(C_6−C_1−C_2)	119.2	120.2	118.8	118.6
ϑ(C_1−S−Me)	103.6	106.8	104.2	103.9

[a] Bond lengths in pm and angles in deg from UB3LYP/6-31G* optimizations.

pH 3.5 to 5.5 until a plateau is reached between pH 5.5 and 7.5. The $G(CO_2)$ yields measured on the plateau account for ca. 40% of the available •OH radicals.

Contributions from Density Functional Theory. DFT calculations provide a convenient and reliable method to determine the structures of both the precursor thioanisoles and the transient radical species derived from them in the course of the radiolysis. Thioanisole itself is predicted (B3LYP/6-31G*) to have a planar heavy-atom framework in accord with a previous report[61] but at odds with results from an optimization at the Hartree−Fock (HF) level,[62] which found this structure to be a transition state. However, the torsional barrier around the ring-sulfur bond is calculated (again B3LYP/6-31G*) to be only 2 kJ mol^{-1}. Chart 1 collects the radicals investigated theoretically and illustrates the numbering system employed. Important bond lengths and angles from (U)B3LYP/6-31G* optimizations are summarized in Table 1 for thioanisole, its (sulfur-centered) radical cation (**1a**), the cyclohexadienyl radical formed by H atom addition at the 4-position (a particular case of **3a**), and the hydroxycyclohexadienyl radical formed via •OH attack at the same site (a particular case of **2a**). The aromatic to dienyl conversion upon H or OH adduct formation is clearly evident from these data; the bond lengths between C_2−C_3 and C_5−C_6 are much reduced, and the oxidation to produce the radical cation shortens the ring-sulfur bond considerably and opens the angle subtended at the sulfur by the substituent methyl group. The sulfur-centered radical cation (^{2}A″ symmetry) is formed by loss of an electron from an orbital with strong π-antibonding character. Note also that the torsional barrier to rotation about the ring-sulfur bond has increased dramatically to 80 kJ mol^{-1} in the cation.

Some results of the natural population analysis are presented in Table 2 for all of these species, and it is clear that the radical cation is indeed sulfur-centered, though some charge is delocalized onto the ring, particularly at the 4-position. The gross difference between the values at C_4 for the cyclohexadienyls reflects the polarity of the CO bond in the hydroxy compound. The Mulliken spin populations at the heavy atoms are listed in Table 3 for the radicals and show typical alternating patterns

TABLE 2: Natural Charges[a] in Thioanisole and Some Radiolytically Derived Transients

	neutral	radical cation	4-OH adduct	4-H adduct
ρ(S)	0.29	0.72	0.34	0.32
ρ(C_1)	−0.19	−0.22	−0.21	−0.22
ρ(C_2)	−0.24	−0.16	−0.27	−0.26
ρ(C_3)	−0.22	−0.22	−0.22	−0.19
ρ(C_4)	−0.25	−0.09	0.01	−0.53
ρ(C_5)	−0.22	−0.20	−0.21	−0.18
ρ(C_6)	−0.26	−0.20	−0.29	−0.28

[a] Natural charges on the heavy-atom framework from NBO analysis.

TABLE 3: Mulliken Spin Populations in Some Transient Radicals from Thioanisole

	radical cation	4-OH adduct	4-H adduct
ρ^s(S)	0.49	0.11	0.09
ρ^s(C_1)	0.08	0.48	0.51
ρ^s(C_2)	0.17	−0.18	−0.19
ρ^s(C_3)	−0.10	0.35	0.37
ρ^s(C_4)	0.31	−0.04	−0.07
ρ^s(C_5)	−0.05	0.41	0.43
ρ^s(C_6)	0.11	−0.20	−0.21

TABLE 4: Optical Absorption Peaks[a] and Dipole Oscillator Strengths in Some Transient Radicals from Thioanisole

	radical cation	4-OH adduct	4-H adduct
λ_{max}	490, 297	368	345
f_{dip}	0.011, 0.019	0.112	0.093

[a] λ_{max} (nm) from TD-UB3LYP/6-31+G(d,p) calculations at the UB3LYP/6-31G* geometries.

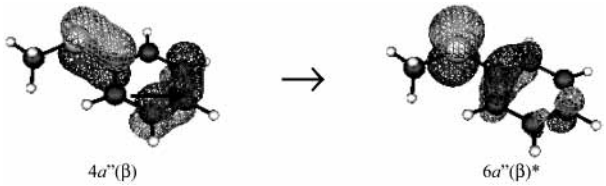

Figure 9. Orbitals involved in visible absorption in the thioanisole radical cation, **1a**.

(large, positive/small, negative) for the substituted species, while the spin on the radical cation is mainly on the sulfur and C_4. Various attempts to locate a ring-centered radical cation (starting from deprotonated cyclohexadienyls, for example) led uniformly to the sulfur-centered radical cation discussed above.

Time-dependent density functional theory (TD-DFT) calculations with the extended 6-31+G(d,p) basis set, carried out at the above DFT geometries, provide strong support for the proposed assignments of the transient spectra. Peaks of optical absorption, together with dipole oscillator strengths, are presented in Table 4 for the radical cation and the substituted radicals. Solvent effects (not included here) will be more pronounced for the charged species. An analysis of the TD-DFT calculations on the radical cation indicates that the transition in the visible is principally $\pi \rightarrow \pi^*$ in the β space involving the orbitals depicted in Figure 9.•

Discussion

•OH-Induced Oxidation of Thioanisole. There is one striking result that must be considered in any discussion of the mechanism of the •OH-induced oxidation of thioanisole. The one-electron oxidation of thioanisole at high proton concentrations (≥0.1 M) leads to the quantitative formation of monomeric sulfur-centered radical cations (Ph−S$^{+\bullet}$−CH_3) equal to ∼100% of the available •OH radicals. On the other hand, at low proton

SCHEME 1

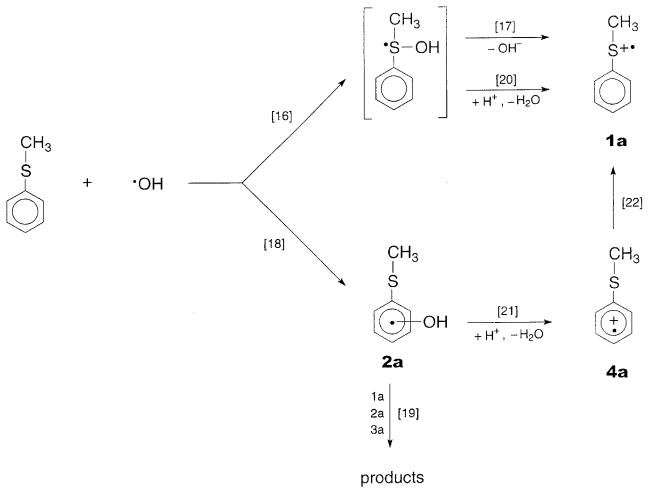

concentration ($\leq 10^{-6}$ M) the one-electron oxidation of thioanisole leads to the formation of the $Ph-S^{+\bullet}-CH_3$ with the radiation chemical yield that accounts for only ca. 55% of the available •OH radicals. The facile explanation of this phenomenon would be that the •OH-addition pattern (thioether functionality vs benzene ring) is pH-dependent. However, this cannot be the case because the state of protonation of both the thioether function and the benzene ring remains the same over the pH range investigated. Thus, this cannot account for the observed •OH addition pattern.

Mechanism. The following mechanism accounts for all of the experimental results presented in this work. In particular, it accounts for the fact that the radiation chemical yields of monomeric sulfur radical cations (**1a**), normalized to the total initial radiation chemical yield of •OH radicals at the given pH, are different on going from low to high pH. In general, the first step in the reaction of •OH radicals with thioethers involves an addition to the sulfur leading to hydroxysulfuranyl-type radicals (Scheme 1, reaction 16), which are characterized by an optical absorption spectrum in the 330−340-nm range.[16,28,63,64] At low proton concentrations, decomposition of the hydroxysulfuranyl radical occurs by a unimolecular dissociation leading to **1a** (Scheme 1, reaction 17). This reaction channel provides the basis for the observation of **1a** with ∼55% efficiency relative to the yield of •OH radicals at the neutral pH (6.7). Under our experimental conditions, reaction 17 is likely very fast because we were not able to assign positively any absorption band to the hydroxysulfuranyl radical on the submicrosecond time scale. Moreover, its detection might be very difficult because of the overlap of different absorptions in this wavelength region. One of the most important reactions between aromatic compounds and •OH radicals is their addition to aromatic rings resulting in the formation of hydroxycyclohexadienyl radicals.[60,65−67] The formation of the hydroxycyclohexadienyl radical (**2a**) with its characteristic absorption band maximum ($\lambda_{max} = 365$ nm and $\epsilon_{365} = 4700\ M^{-1}\ cm^{-1}$) was observed in the transient spectrum (Figure 3) recorded at pH 6.7. This observation indicates that there is a second competitive reaction pathway for the reaction of •OH radicals with thioanisole (Scheme 1, reaction 18). This reaction pathway accounts for ∼45% of the total yield of the •OH radicals at pH 6.7. The same absorption band ($\lambda_{max} = 365$ nm) was observed by Mohan and Mittal,[35] as well; however, it was assigned to the •OH adduct at the thioether functionality. The **2a** radicals decay subsequently through radical−radical reactions (Scheme 1, reaction 19) that likely involve **1a** radical cations and cyclohexadienyl-type radicals (**2a** and **3a**).[58,60] One might also expect that hydroxyl radicals can abstract hydrogen atoms from the methyl site of thioanisole that leads to the formation of the $Ph-S-CH_2^{\bullet}$ radicals. These radicals are characterized by an optical absorption with λ_{max} located at 330 nm (see Figures 6 and 7, curves b). The radical balance performed suggests that this reaction channel is insignificant. Moreover, its detection might be very difficult because of the overlap of the $Ph-S-^{\bullet}CH_2$ absorption with absorptions of different transients in this wavelength region.

At high proton concentrations, decomposition of the hydroxysulfuranyl radical occurs through external proton catalysis and hydroxide elimination, leading to **1a** and water (Scheme 1, reaction 20). Typical rate constants for such reactions are on the order of $2 \times 10^{10}\ M^{-1}\ s^{-1}$.[16,28] We have to rationalize, however, that the radiation chemical yield of **1a** accounts for ∼100% of the total yield of the •OH radicals at pH 0. A reasonable assumption is (vide supra) that the •OH-addition pattern (thioether functionality vs benzene ring) should not be pH-dependent. This, in turn, eliminates the hydroxysulfuranyl radical as a direct precursor of the remaining 45% of **1a**. Consequently, •OH radicals are able to undergo addition to the aromatic ring in very acidic solutions leading to **2a** (Scheme 1, reaction 18). As it was pointed out by several groups,[58−60,68−70] the •OH adducts to the aromatic ring undergo an acid-catalyzed elimination of the hydroxide ions (with the rate constants on the order of $\sim 10^9\ M^{-1}\ s^{-1}$),[58−60] leading to the formation of the corresponding radical cations and water. At pH 0, such a transformation of **2a** into the corresponding radical cation (Scheme 1, reaction 21) with the delocalized positive charge on the aromatic ring ($Ph^{+\bullet}-S-CH_3$) (**4a**) is expected to occur on the nanosecond time scale with a half-life of $t_{1/2} \approx 7$ ns. A close inspection of the absorption spectrum in the UV−visible range (Figure 4) does not reveal any additional absorption bands that might be assigned to **4a**. Other than the bands assigned to **1a**, the only other band observed was the strong absorption band with maximum at $\lambda = 365$ nm assigned to **3a**. This finding can be rationalized in terms of the highly unstable nature of the **4a** radical cations. From this analysis and remembering that the yield of **1a** is 100% of the •OH radicals, it is reasonable to conclude that **4a** undergoes a very rapid conversion into a **1a** radical cation (Scheme 1, reaction 22). Indeed, as pointed out above, an extensive search by DFT calculations failed to find a stable minimum in which the positive charge was principally delocalized on the aromatic ring.

Structures **1a** and **4a** are meant to represent actual chemical structures and not resonance structures. They would be resonance structures if the nuclear configurations were the same. However, for the purpose of discussing the nature of the radical cations of thioanisole, **1a** and **4a** should be thought of as physical entities with their dominant electronic configurations as indicated but with each of their nuclear configurations relaxed with respect to their respective electronic configurations.

•OH-Induced Oxidation of Phenylthioacetic Acid. It is noteworthy that there is a progressive decrease in $G(CO_2)$ (Figure 8) on going from pH 3.5 to 5.5 until a plateau is reached between pH 5.5 and 7.5. In principle, this behavior can be rationalized by the mechanism displayed in Scheme 1 for TA; however, there are certain differences, which are of significance in understanding the pH effects on the transient absorption spectra. Oxidation of phenylthioacetic acid by •OH radicals at high pH (Scheme 2, reactions 23 and 24), as well as at low pH (reactions 23 and 25), leads in general to the formation of unstable radicals, $Ph-S^{+\bullet}-CH_2-COO^-(H^+)$, (**1b**). These radicals undergo efficient decarboxylation (Scheme 2, reaction 26),

SCHEME 2

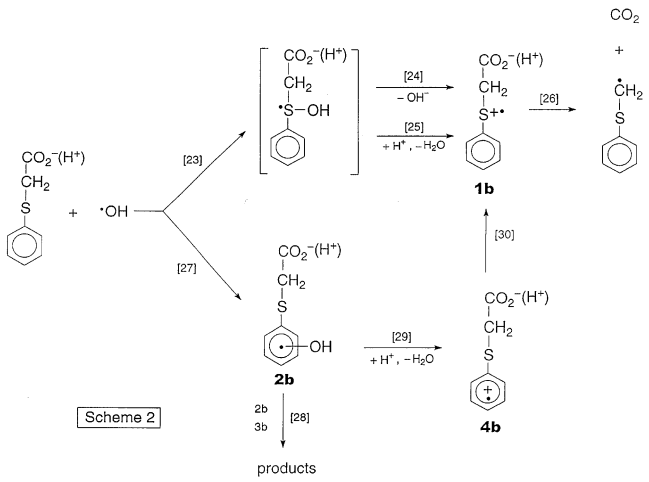

as it is indicated by the formation of Ph−S−C•H$_2$ radicals and CO_2.

The $G(CO_2)$ measured on the plateau between pH 5.5 and 7.5 is an excellent probe for estimating the extent of •OH addition to the thioether functionality in phenylthioacetic acid in the given pH range (Scheme 2, reaction 23). This yield of decarboxylation accounts for only half of the available •OH radicals in the pH range of 5.5 to 7.5, and this value for the yield is in excellent agreement with the value of 55% calculated in thioanisole (vide supra). Thus, the fraction of •OH radicals reacting by addition to the aromatic ring of PTAA and resulting in the formation of hydroxycyclohexadienyl type radicals (**2b**) (Scheme 2, reaction 27) can be taken to be equal to 50%, as well. This is consistent with the previous discussion where it was necessary to take into account contributions from **2b** and from ∼10% of the cyclohexadienyl-type radicals (**3b**) to the overall absorptions at $\lambda = 330$ nm, and $\lambda = 360$ nm.

A similar approach can be used for the quantification of the absorption spectrum obtained at pH 1. As before, it is assumed (vide supra) that the •OH-addition pattern (thioether functionality vs benzene ring) should not be pH-dependent. The measured $G(CO_2)$ yields, which account for ca. 80−90% of the available •OH radicals, can be rationalized by a similar sequence of reactions to those proposed earlier for thioanisole (Scheme 1, reactions 21 and 22). The additional yield of CO_2 at pH 1 comes through the formation of a highly unstable radical cation with its delocalized positive charge on the aromatic ring (**4b**) (Scheme 2, reaction 29) and its subsequent rapid transformation into **1b** (Scheme 2, reaction 30).

A brief explanation is necessary to rationalize the sigmoidal $G(CO_2)$ vs pH profile between pH 3 and 7 with the half-value of ∼4.3 (Figure 8). Because the formation of CO_2 (via •OH addition to aromatic ring pathway) depends primarily on the competition between reactions 28 and 29 (Scheme 2), we believe that their rates appear to be equal at this pH, that is, at $[H^+] =$ ca. 5.0×10^{-5} M. Assuming $k_{29} = \sim 10^9$ M^{-1} s^{-1},[58−60] this would mean $k_{28} = 5.0 \times 10^4$ s^{-1}.

We are now left with the question whether the values of optical densities (ΔOD_{330} and ΔOD_{360}) taken from the absorption spectra displayed in Figures 6 and 7 can be reconstructed from the ϵ's and yields of the presumed transients and thus confirm the validity of the proposed mechanism. These two wavelengths ($\lambda = 330$ and 360 nm) were chosen because they represent the location of the absorption maxima of the three key transients (**2b**, **3b**, and Ph−S−•CH$_2$ radicals) of which the relative contributions to the overall absorption spectra were very sensitive to pH. The reconstruction of ΔOD_{330} and ΔOD_{360} was done by using the computed values of $\epsilon_{330} = 4200$ M^{-1} cm^{-1} for Ph−S−•CH$_2$ and $\epsilon_{360} = 4700$ (6200) M^{-1} cm^{-1} for **2b** (**3b**). The values taken for **2b** and **3b** were the same as the ones determined for **2a** and **3a**, respectively. The contributions to ΔOD_{360} by Ph−S−•CH$_2$ and to ΔOD_{330} by **2b** and **3b** were computed in a manner similar to that used for the spectral computations on thioanisole (vide supra). The yields were taken to be according to Scheme 2. The absorbances computed were in good agreement with the actual experimental data.

Conclusions

The results from this study show that hydroxyl radicals (•OH) react with thioanisole (TA) and its carboxylic derivative phenylthioacetic acid (PTAA) via two competitive addition pathways, with the thioether functionality and with the aromatic ring, which lead to the formation of monomeric sulfur radical cations (Ph−S$^{+\bullet}$−R) and hydroxycyclohexadienyl radicals (Ph•−(OH)−S−R), respectively. At low pH, •OH addition, both to the thioether functionality and to the aromatic ring, leads only to the Ph−S$^{+\bullet}$−R radical cations. This paper provides no evidence, either theoretical or experimental, that radical cations derived from aromatic thioethers with delocalized positive charge on the aromatic ring (Ph$^{+\bullet}$−S−R) are observable. Rather they convert rapidly into monomeric sulfur radical cations (Ph−S$^{+\bullet}$−R).

Acknowledgment. This work was supported by the Committee of Scientific Research, Poland (Grant No. 3 TO 9A 037 19) (A.K.-S. and K.B) and by the Office of Basic Energy Sciences of the U.S. Department of Energy (G.L.H. and I.C.). The authors thank Professor K.-D. Asmus for helpful discussions and Mrs. A. Sciegosz for valuable technical assistance. This paper is Document No. NDRL-4368 from the Notre Dame Radiation Laboratory.

References and Notes

(1) Wrzyszczynski, A.; Scigalski, F.; Paczkowski, J. *Nukleonika* **2000**, *45*, 73−81.

(2) Chatgilialoglu, C.; Bertrand, M. P.; Ferreri, C. Sulfur-centered radicals in organic synthesis. In *S-centered radicals*; Alfassi, Z. B., Ed.; John Wiley & Sons Ltd.: Chichester, U.K., 1999; pp 311−354.

(3) Bauld, N. L.; Aplin, J. T.; Yueh, W.; Loinaz, A. *J. Am. Chem. Soc.* **1997**, *119*, 11381−11389.

(4) Tobien, T.; Cooper, W. J.; Nickelsen, M. G.; Pernas, E.; O'Shea, K. E.; Asmus, K.-D. *Environ. Sci. Technol.* **2000**, *34*, 1286−1291.

(5) Urbanski, S. P.; Wine, P. H. Chemistry of Gas-Phase Organic Sulfur-centered Radicals. In *S-centered Radicals*; Alfassi, Z. B., Ed.; John Wiley & Sons Ltd.: Chichester, U.K., 1999; pp 97−140.

(6) Speight, V. L.; Balchon, E. R.; Nixon, E. M. *Fla. Water Resour. J.* **1997**, 25−26.

(7) Wardman, P. Thiyl Radicals in Biology: Their Role as a 'Molecular Switch' central to Cellular Oxidative Stress. In *S-centered Radicals*; Alfassi, Z. B., Ed.; John Wiley & Sons Ltd.: Chichester, U.K., 1999; pp 289−309.

(8) Ozaki, S.; Ortiz de Montelano, P. R. *J. Am. Chem. Soc.* **1995**, *117*, 7056−7064.

(9) Asmus, K.-D. Heteroatom-centered free radicals. Some selected contributions by radiation chemistry. In *Radiation Chemistry*: *Present Status and Future Prospects*; Jonah, C., Ed.; Elsevier: Amsterdam, 2000.

(10) Asmus, K.-D. *Nukleonika* **2000**, *45*, 3−10.

(11) Asmus, K.-D.; Bonifacic, M. Sulfur-centered reactive intermediates as studied by radiation chemical and complementary techniques. In *S−Centered Radicals*; Alfassi, Z. B., Ed.; John Wiley & Sons Ltd.: Chichester, U.K., 1999; pp 141−191.

(12) Asmus, K.-D. Sulfur-centered three-electron bonded radical species. In *Sulfur-Centered Reactive Intermediates in Chemistry and Biology*; Chatgilialoglu, C., Asmus, K.-D., Eds.; Plenum Press: New York, 1990; Vol. 197, pp 155−172.

(13) Asmus, K.-D. *Acc. Chem. Res.* **1979**, *12*, 436−442.

(14) Gilbert, B. C. Structure and reaction mechanisms in sulphur-radical chemistry revealed by e.s.r. spectroscopy. In *Sulfur-Centered Reactive*

Intermediates in Chemistry and Biology; Chatgilialoglu, C., Asmus, K.-D., Eds.; Plenum Press: New York, 1990; Vol. 197, pp 135−154.
(15) Gilbert, B. C.; Hodgeman, D. K. C.; Norman, R. O. C. *J. Chem. Soc., Perkin Trans. 2* **1973**, 1748−1753.
(16) Schöneich, C.; Bobrowski, K. *J. Am. Chem. Soc.* **1993**, *115*, 6538−6547.
(17) Mönig, J.; Goslich, R.; Asmus, K.-D. *Ber. Bunsen-Ges. Phys. Chem.* **1986**, *90*, 115−121.
(18) Göbl, M.; Bonifacic, M.; Asmus, K.-D. *J. Am. Chem. Soc.* **1984**, *106*, 5984−5988.
(19) Bonifacic, M.; Möckel, H.; Bahnemann, D.; Asmus, K.-D. *J. Chem. Soc., Perkin Trans. 2* **1975**, 675−685.
(20) Marciniak, B.; Andrzejewska, E.; Hug, G. L. *J. Photochem. Photobiol. A.* **1998**, *112*, 21−28.
(21) Bobrowski, K.; Hug, G. L.; Marciniak, B.; Miller, B. L.; Schöneich, C. *J. Am. Chem. Soc.* **1997**, *119*, 8000−8011.
(22) Bobrowski, K.; Marciniak, B.; Hug, G. L. *J. Photochem. Photobiol. A* **1994**, *81*, 159−168.
(23) Carmichael, I. *Nukleonika* **2000**, *45*, 11−17.
(24) Clark, T. The electronic properties of sulphur-containing substituents and molecules: an ab initio study. In *Sulfur-Centered Reactive Intermediates in Chemistry and Biology*; Chatgilialoglu, C., Asmus, K.-D., Eds.; Plenum Press: New York, 1990; Vol. 197, pp 13−18.
(25) Bobrowski, K.; Hug, G. L.; Marciniak, B.; Schöneich, C.; Wisniowski, P. *Res. Chem. Intermed.* **1999**, *25*, 285−297.
(26) Bobrowski, K.; Pogocki, D.; Schöneich, C. *J. Phys. Chem. A* **1998**, *102*, 10512−10521.
(27) Schöneich, C.; Zhao, F.; Madden, K. P.; Bobrowski, K. *J. Am. Chem. Soc.* **1994**, *116*, 4641−4652.
(28) Bobrowski, K.; Schöneich, C. *J. Chem. Soc., Chem. Commun.* **1993**, 795−797.
(29) Schöneich, C.; Aced, A.; Asmus, K.-D. *J. Am. Chem. Soc.* **1993**, *115*, 11376−11383.
(30) Bobrowski, K.; Holcman, J. *J. Phys. Chem.* **1989**, *93*, 6381−6387.
(31) Yokoi, H.; Hatta, A.; Ishiguro, K.; Sawaki, Y. *J. Am. Chem. Soc.* **1998**, *120*, 12728−12733.
(32) Yagci, Y.; Schnabel, W.; Wilpert, A.; Bendig, J. *J. Chem. Soc., Faraday Trans.* **1994**, *90*, 287−291.
(33) Sumiyoshi, T.; Kawasaki, M.; Katayama, M. *Bull. Chem. Soc. Jpn.* **1993**, *66*, 2510−2514.
(34) Ioele, M.; Steenken, S.; Baciocchi, E. *J. Phys. Chem. A* **1997**, *101*, 2979−2987.
(35) Mohan, H.; Mittal, J. P. *J. Phys. Chem. A* **1997**, *101*, 10012−10017.
(36) Gawandi, V. B.; Mohan, H.; Mittal, J. P. *Phys. Chem. Chem. Phys.* **1999**, *1*, 1919−1926.
(37) Engman, L.; Lind, J.; Merenyi, G. *J. Phys. Chem.* **1994**, *98*, 3174−3182.
(38) Sumiyoshi, T.; Sakai, H.; Kawasaki, M.; Katayama, M. *Chem. Lett.* **1992**, 617−620.
(39) Jonsson, M.; Lind, J.; Merenyi, G.; Eriksen, T. E. *J. Chem. Soc., Perkin Trans. 2* **1995**, 67−70.
(40) Hug, G. L.; Wang, Y.; Schöneich, C.; Jiang, P.-Y.; Fessenden, R. W. *Radiat. Phys. Chem.* **1999**, *54*, 559−566.
(41) Karolczak, S.; Hodyr, K.; Lubis, R.; Kroh, J. *J. Radioanal. Nucl. Chem.* **1986**, *101*, 177−190.
(42) Karolczak, S.; Hodyr, K.; M., P. *Radiat. Phys. Chem.* **1992**, *39*, 1−8.
(43) Janata, E.; Schuler, R. H. *J. Phys. Chem.* **1982**, *86*, 2078−2084.
(44) von Sonntag, C. *The Chemical Basis of Radiation Biology*; Taylor and Francis: New York, 1987.
(45) Fricke, H.; Hart, E. J. In *Radiation Dosimetry*; Attix, T. H., Roesch, W. C., Eds.; Academic Press: New York, 1966.
(46) Schuler, R. H.; Hartzell, A. L.; Behar, B. *J. Phys. Chem.* **1981**, *85*, 192−199.
(47) Buxton, G. V.; Greenstock, C. L.; Helman, W. P.; Ross, A. B. *J. Phys. Chem. Ref. Data* **1988**, *17*, 513−886.
(48) Frisch, M. J.; Trucks, G. W.; Schlegel, H. B.; Scuseria, G. E.; Robb, M. A.; Cheeseman, J. R.; Zakrzewski, V. G.; Montgomery, J. A., Jr.; Stratmann, R. E.; Burant, J. C.; Dapprich, S.; Millam, J. M.; Daniels, A. D.; Kudin, K. N.; Strain, M. C.; Farkas, O.; Tomasi, J.; Barone, V.; Cossi, M.; Cammi, R.; Mennucci, B.; Pomelli, C.; Adamo, C.; Clifford, S.; Ochterski, J.; Petersson, G. A.; Ayala, P. Y.; Cui, Q.; Morokuma, K.; Malick, D. K.; Rabuck, A. D.; Raghavachari, K.; Foresman, J. B.; Cioslowski, J.; Ortiz, J. V.; Stefanov, B. B.; Liu, G.; Liashenko, A.; Piskorz, P.; Komaromi, I.; Gomperts, R.; Martin, R. L.; Fox, D. J.; Keith, T.; Al-Laham, M. A.; Peng, C. Y.; Nanayakkara, A.; Gonzalez, C.; Challacombe, M.; Gill, P. M. W.; Johnson, B. G.; Chen, W.; Wong, M. W.; Andres, J. L.; Head-Gordon, M.; Replogle, E. S.; Pople, J. A. *Gaussian 98*, revision A.7; Gaussian, Inc.: Pittsburgh, PA, 1998.
(49) Becke, D. A. *J. Chem. Phys.* **1993**, *98*, 5648−5652.
(50) Slater, J. C. *The Self-Consistent Field for Molecules and Solids*; McGraw-Hill: New York, 1974.
(51) Becke, A. D. *ACS Symp. Ser.* **1989**, *394*, 165−179.
(52) Vosko, S. H.; Wilk, L.; Nusair, M. *Can. J. Phys.* **1980**, *58*, 1200−1211.
(53) Lee, C.; Yang, W.; Parr, R. G. *Phys. Rev. B* **1988**, *37*, 785−789.
(54) Hariharan, P. C.; Pople, J. A. *Chem. Phys. Lett.* **1972**, *16*, 217−219.
(55) Casida, M. E.; Jamorski, C.; Casida, K. C.; Salahub, D. R. *J. Chem. Phys.* **1998**, *108*, 4439−4449.
(56) Reed, A. E.; Weinstock, R. B.; Weinhold, F. *J. Chem. Phys.* **1985**, *83*, 735−746.
(57) Neta, P.; Huie, R. E.; Ross, A. B. *J. Phys. Chem. Ref. Data* **1988**, *17*, 1027.
(58) O'Neill, P.; Steenken, S.; Schulte-Frohlinde, D. *J. Phys. Chem.* **1977**, *81*, 31−34.
(59) Sehested, K.; Holcman, J.; Hart, E. J. *J. Phys. Chem.* **1977**, *81*, 1363−1367.
(60) O'Neill, P.; Steenken, S.; Schulte-Frohlinde, D. *J. Phys. Chem.* **1975**, *79*, 2773−2779.
(61) Dolgounitcheva, O.; Zakrzewski, V. G.; Ortiz, J. V.; Ratovski, G. V. *Int. J. Quantum Chem.* **1998**, *70*, 1037−1043.
(62) Dal Colle, M.; Distefano, G.; Jones, D.; Modelli, A. *J. Phys. Chem. A* **2000**, *104*, 8227−8235.
(63) Bobrowski, K.; Pogocki, D.; Schöneich, C. *J. Phys. Chem.* **1993**, *97*, 13677−13684.
(64) Asmus, K.-D.; Bahnemann, D.; Bonifacic, M.; Gillis, H. A. *Discuss. Faraday Chem. Soc.* **1975**, *63*, 213−235.
(65) Pan, X.-M.; Schuchmann, M. N.; von Sonntag, C. *J. Chem. Soc., Perkin Trans. 2* **1993**, 289−297.
(66) Sehested, K.; Corfitzen, H.; Christensen, H. C.; Hart, E. J. *J. Phys. Chem.* **1975**, *79*, 310−315.
(67) Gordon, S.; Schmidt, K. H.; Hart, E. J. *J. Phys. Chem.* **1977**, *81*, 104−109.
(68) Sehested, K.; Holcman, J. *Nukleonika* **1979**, *24*, 941−950.
(69) Zevos, N.; Sehested, K. *J. Phys. Chem.* **1978**, *82*, 138−141.
(70) Sehested, K.; Hart, E. J. *J. Phys. Chem.* **1975**, *79*, 1639−1642.